

On the analysis of delamination in multilayered inhomogeneous rods under torsion

Victor I. Rizov*

*Department of Technical Mechanics, University of Architecture, Civil Engineering and Geodesy,
1 Chr. Smirnensky blvd., 1046 – Sofia, Bulgaria*

(Received June 3, 2019, Revised August 12, 2019, Accepted August 28, 2019)

Abstract. The present paper is focused on analyzing the delamination of inhomogeneous multilayered rods of circular cross-section loaded in torsion. The rods are made of concentric longitudinal layers of individual thickness and material properties. A delamination crack is located arbitrary between layers. Thus, the internal and external crack arms have circular and ring-shaped cross-sections, respectively. The layers exhibit continuous material inhomogeneity in radial direction. Besides, the material has non-linear elastic behavior. The delamination is analyzed in terms of the strain energy release rate. General solution to the strain energy release rate is derived by considering the energy balance. The solution is applied to analyze the delamination of cantilever rod. For verification, the strain energy release rate is derived also by considering the complementary strain energy.

Keywords: multilayered rod; torsion; delamination; material non-linearity; inhomogeneous material

1. Introduction

The inhomogeneous structural members, whose material properties vary continuously within a macro-volume, are widely used in various load-bearing structural applications in different branches of mechanical and civil engineering (Tokovyy and Ma 2008, 2013, Tokova *et al.* 2017, Tokovyy and Ma 2016). The wide-spread usage of inhomogeneous structural materials is due also to their ability to satisfy different structural requirements in different zones of a structural member.

New and advanced classes of inhomogeneous structural materials are functionally graded materials (Gasik 2010, Han *et al.* 2001, Hedia *et al.* 2014, Hirai and Chen 1999, Kawasaki and Watanabe, 1997, Mahamood and Akinlabi, 2017, Markworth *et al.* 1995, Miyamoto *et al.* 1999, Nemat-Allal *et al.* 2011, Saiyathibrahim *et al.* 2016, Shrikantha and Gangadharan 2014). They are made of two or more constituent materials mixed continuously and functionally during manufacturing. The properties of functionally graded materials change smoothly in the volume of a structural member and are functions of spatial position. One of the basic advantages of the functionally graded materials over the conventional homogeneous structural materials is the fact that the microstructure of the functionally graded materials can be tailored so as to meet high performance requirements. Thus, it is not surprising that the application of the functionally graded

*Corresponding author, Professor, E-mail: V_RIZOV_FHE@UACG.BG

materials has been constantly increasing for the last three decades in aerospace, nuclear reactors, electronics and biomedicine.

The frequent use of inhomogeneous materials in various load-bearing engineering structures imposes high requirements with respect to their fracture behavior. Thus, in the last thirty years considerable attention has been paid from the international academic circles to analysis of the fracture behaviour of the inhomogeneous (functionally graded) materials and structures (Carpinteri and Pugno 2006, Dolgov, 2005, 2016, Erdogan, 1995, Tilbrook *et al.* 2005). Being different from the ordinary homogeneous structural members, the fracture analysis of inhomogeneous members possesses some specific characteristics. The most important of them is the fact that the properties of inhomogeneous materials are related to the coordinates which significantly complicates the fracture analysis.

Some problems of fracture behaviour of inhomogeneous (functionally graded) materials have been considered in (Erdogan 1995). Various analyses of fracture have been carried-out assuming linear-elastic mechanical behaviour of the inhomogeneous material. Thus, solutions of crack problems have been derived by applying methods of linear-elastic fracture mechanics. The results obtained can be used by scientists and practicing engineers who are developing methods for design of inhomogeneous structural members and components. Different aspects of surface cracking and debonding of inhomogeneous structures and materials are also considered (Erdogan 1995).

Various studies of fracture behaviour of inhomogeneous (functionally graded) materials have been reviewed in (Tilbrook *et al.* 2005). The influence of microstructural gradation on the fracture has been investigated. Linear-elastic analyses of cracks oriented parallel or perpendicular to the gradient direction have been presented. The analyses have been carried-out by applying linear-elastic fracture mechanics. Solutions for rectilinear and curved cracks have been discussed. Works on fracture behaviour of inhomogeneous materials under fatigue crack loading conditions have also been reviewed. Studies of cracks in linear-elastic inhomogeneous materials under thermal loading have been presented too (Tilbrook *et al.* 2005).

A method for evaluation of the strength of structures composed by functionally graded materials containing cracks has been developed in (Carpinteri and Pugno 2006). The method has been applied successfully on inhomogeneous beams under bending and plates under tension assuming linear-elastic mechanical behaviour of the material. The fracture analyses have been performed at linear variation of the modulus of elasticity of the inhomogeneous material between two given values in the thickness direction of the structural member (Carpinteri and Pugno 2006.)

The above literature review indicates that fracture of inhomogeneous materials and structural members and components has been studied mainly assuming linear-elastic mechanical behavior of the material. Recently, papers which deal with analyses of delamination fracture of inhomogeneous (functionally graded) beams exhibiting material non-linearity has also been published (Rizov, 2018a, b, 2019). However, these papers consider individual analyses of separate beam configurations (Rizov, 2018a, b, 2019). Therefore, the aim of the present paper is to develop general analysis of the delamination fracture of inhomogeneous multilayered rods which exhibit non-linear elastic behavior of the material. The rods have a circular cross-section and are loaded in torsion. The rods are made of concentric longitudinal inhomogeneous layers and have a delamination crack located arbitrary between layers. The fracture is studied in terms of the strain energy release rate. General solution to the strain energy release rate is derived by considering the balance of the energy. The general solution is applied to analyze the delamination in a cantilever rod under torsion. The strain energy release rate is derived also by considering the complementary strain energy for verification.

2. General approach for analyzing of the strain energy release rate

A multilayered rod of circular cross-section of radius, R_A , is shown in Fig. 1.

The rod is made of adhesively bonded concentric longitudinal layers. The number of layers is arbitrary. Each layer has individual thickness and material properties. The material in each layer has non-linear elastic mechanical properties. Besides, each layer exhibits continuous (smooth) material inhomogeneity in radial direction. A delamination crack is located arbitrary between layers. The crack presents a circular cylindrical surface of radius, R_B . Thus, the crack front is a circle of radius, R_B . The internal and external crack arms have circular and ring-shaped cross-section, respectively. The radius of the cross-section of the internal crack arm is R_B . The internal and external radiuses of the cross-section of the external crack arm are R_B and R_A , respectively. The crack length is a . The rod is loaded in torsion by an arbitrary number of torsion moments, T_i . A torsion moment, T_b , is applied at the free end of the internal crack arm. Under these torsion moments, the rod is in a state of equilibrium. The length of the rod is denoted by l .

The delamination fracture behaviour of the rod in Fig. 1 is analyzed in terms of the strain energy release rate, G . For this purpose, general solution to the strain energy release rate is derived by considering the balance of the energy. By assuming a small increase, δa , of the crack length, the balance of the energy is written as

$$\sum_{i=1}^{i=n_T} T_i \delta \psi_i + T_b \delta \psi_b = \frac{\partial U}{\partial a} \delta a + G l_{cf} \delta a \tag{1}$$

where $\delta \psi_i$ is the increases of the angle of twist of the rod cross-section in which the i -th torsion moment is applied, $\delta \psi_b$ is the increase of the angle of twist of the free end of the internal crack arm, n_T is the number of torsion moments, U is the strain energy stored in the rod and l_{cf} is the length of the crack front. From (1), G is expressed as

$$G = \sum_{i=1}^{i=n_T} \frac{T_i}{l_{cf}} \frac{\partial \psi_i}{\partial a} + \frac{T_b}{l_{cf}} \frac{\partial \psi_b}{\partial a} - \frac{1}{l_{cf}} \frac{\partial U}{\partial a} \tag{2}$$

Since

$$l_{cf} = 2\pi R_B \tag{3}$$

Eq. (2) is re-written as

$$G = \sum_{i=1}^{i=n_T} \frac{T_i}{2\pi R_B} \frac{\partial \psi_i}{\partial a} + \frac{T_b}{2\pi R_B} \frac{\partial \psi_b}{\partial a} - \frac{1}{2\pi R_B} \frac{\partial U}{\partial a} \tag{4}$$

By using the integrals of Maxwell-Mohr, the angle of twist, ψ_i , is obtained as

$$\psi_i = \sum_{j=1}^{j=m-1} T_{ij} \frac{\gamma_j}{R_A} (l_{j+1} - l_j) + T_{iCD} \frac{\gamma_{CD}}{R_A} (a - l_m) + T_{iDP} \frac{\gamma_{DP}}{R_A} (s_1 - a) + \sum_{k=1}^{k=q-1} T_{ik} \frac{\gamma_k}{R_A} (s_{k+1} - s_k) \tag{5}$$

where m and q are the numbers of torsion moments applied on the external crack arm and the un-cracked rod part ($a \leq x \leq l$), γ_j is the shear strain at the periphery of the rod in the j -th portion of the external crack arm, γ_{CD} is the shear strain at the periphery of the rod in portion, CD , of the external

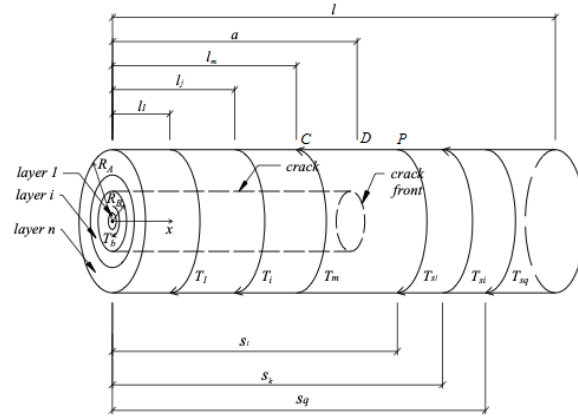


Fig. 1 Multilayered inhomogeneous rod with a delamination circular cylindrical crack loaded in torsion

crack arm, γ_{DP} is the shear strain at the periphery of the rod in portion, DP , of the un-cracked part of the rod, γ_k is the shear strain at the periphery of the rod in the k -th portion of the un-cracked part of the rod, T_{ij} , T_{iCD} , T_{iDP} and T_{ik} are, respectively, the torsion moments induced by the unit loading for obtaining of ψ_i in the j -th portion of the external crack arm, portion, CD , of the external crack arm, portion, DP , of the un-cracked part of the rod and the k -th portion of the un-cracked part of the rod, l_j and s_k are the abscissas of the cross-sections in which torsion moments, T_i and T_{s_i} , are applied.

The angle of twist of the free end of the internal crack arm is found as

$$\psi_b = T_\eta \frac{\gamma_{br}}{R_B} a + T_{DP} \frac{\gamma_{DP}}{R_A} (s_1 - a) + \sum_{k=1}^{k=q-1} T_k \frac{\gamma_k}{R_A} (s_{k+1} - s_k) \tag{6}$$

where γ_{br} is the shear strain at the periphery of the internal crack arm, T_η , T_{DP} and T_k are, respectively, the torsion moments induced by the unit loading for obtaining of ψ_b in the internal crack arm, portion, DP , of the un-cracked part of the rod and the k -th portion of the un-cracked part of the rod.

The strain energy in the rod is expressed as

$$U = U_{br} + U_{vn} + U_{nc} \tag{7}$$

where U_{br} , U_{vn} and U_{nc} are the strain energies stored in the internal and external crack arms, and in the un-cracked portion of the rod, respectively.

The strain energy in the internal crack arm is written as

$$U_{br} = \sum_{i=1}^{i=n_b} \int_{0R_{i-1}}^a \int_{R_{i-1}}^{R_i} \int_0^{2\pi} u_{0br_i} R dx dR d\varphi \tag{8}$$

where u_{0br_i} is the strain energy density in the i -th layer of the internal crack arm, n_b is the number of layers in the internal crack arm, R_{i-1} and R_i are the radiuses of internal and external surfaces of the i -th layer, R and φ are the polar coordinates.

The mechanical behaviour of the material in the i -th layer is treated by non-linear stress-strain relation written in a general form

$$\tau_i = \tau_i(\gamma) \tag{9}$$

where τ_i and γ are the shear stress and strain, respectively. The strain energy density, u_{0br_i} , is obtained by integrating of (9)

$$u_{0br_i} = \int_0^\gamma \tau_i(\gamma) d\gamma \tag{10}$$

The strain energy in the external crack arm is written as

$$U_{vn} = \sum_{i=1}^{i=n_v} \sum_{j=1}^{j=m} \int_{l_{j-1}R_{i-1}}^{l_j R_i} \int_0^{2\pi} u_{0vn_{ij}} R dx dR d\varphi + \sum_{i=1}^{i=n_v} \int_{l_m R_{i-1}}^a \int_0^{2\pi} u_{0vn_{im+1}} R dx dR d\varphi \tag{11}$$

where $u_{0vn_{ij}}$ is the strain energy density in the i -th layer of the j -th portion of the external crack arm, $u_{0vn_{im+1}}$ is the strain energy density in the i -th layer of portion, CD , of the external crack arm, n_v is the number of layers in the external crack arm. The strain energy densities, $u_{0vn_{ij}}$ and $u_{0vn_{im+1}}$, are obtained, respectively, by replacing of τ_i with τ_{ij} and τ_{im+1} in (10). Here, τ_{ij} is the shear stress in the i -th layer of the j -th portion of the external crack arm, τ_{im+1} is the shear stress in the i -th layer of portion, CD , of the external crack arm.

The strain energy in the un-cracked part of the rod is expressed as

$$+ \sum_{i=1}^{i=n_{nc}} \sum_{j=2}^{j=s_q} \int_{s_{j-1}R_{i-1}}^{s_j R_i} \int_0^{2\pi} u_{0nc_{ij}} R dx dR d\varphi \tag{12}$$

where $u_{0nc_{i1}}$ is the strain energy density in the i -th layer of portion, DP , of the un-cracked part of the rod, $u_{0nc_{ij}}$ is the strain energy density in the i -th layer of the j -th portion of the un-cracked part of the rod (these strain energy densities are obtained by replacing of τ_i with τ_{i1} and τ_{ij} in (10) where τ_{i1} is the shear stress in i -th layer of portion, DP , of the un-cracked part of the rod, τ_{ij} is the shear stress in i -th layer of the j -th portion of the un-cracked part of the rod), n_{nc} is the number of layers in the un-cracked part of the rod.

The following general solution for the strain energy release rate for the delamination crack in the inhomogeneous multilayered rod shown in Fig. 1 is derived by substituting of (5), (6), (7), (8), (11) and (12) in (4)

$$G = \sum_{i=1}^{i=n_r} \frac{T_i}{2\pi R_B} \left(T_{iCD} \frac{\gamma_{CD}}{R_A} - T_{iDP} \frac{\gamma_{DP}}{R_A} \right) + \frac{T_b}{2\pi R_B} \left(T_\eta \frac{\gamma_{br}}{R_B} - T_{DP} \frac{\gamma_{DP}}{R_A} \right) - \frac{1}{2\pi R_B} \left[\sum_{i=1}^{i=n_b} \int_{R_{i-1}}^{R_i} \int_0^{2\pi} u_{0br_i} R dx d\varphi + \sum_{i=1}^{i=n_v} \int_{R_{i-1}}^{R_i} \int_0^{2\pi} u_{0vn_{im+1}} R dx d\varphi - \sum_{i=1}^{i=n_{nc}} \int_{R_{i-1}}^{R_i} \int_0^{2\pi} u_{0nc_{i1}} R dx d\varphi \right] \tag{13}$$

The integration in (13) should be performed by the MatLab computer program for particular rod geometry and loading conditions. The shear strain, γ_{br} , that participates in (13) is obtained from

the following equation for equilibrium of the cross-section of the internal crack arm

$$T_b = \sum_{i=1}^{i=n_b} \int_{R_{i-1}}^{R_i} \int_0^{2\pi} \tau_i R dR d\varphi \quad (14)$$

In (14), the shear stress, τ_i , is presented as a function of shear strain, γ , by using the stress-strain relation (9). The distribution of the shear strain in the cross-section of the internal crack arm is treated by applying the Bernoulli's hypothesis for plane sections since rods of high length to diameter ratio are considered in the present paper

$$\gamma = \frac{\gamma_{br}}{R_B} R \quad (15)$$

where

$$0 \leq R \leq R_B \quad (16)$$

After substituting of (9) and (15) in (14), the equation should be solved with respect to γ_{br} by using the MatLab computer program.

The shear strain, γ_{CD} , that is involved in (13) is obtained from the following equation for equilibrium of the cross-section of the external crack arm in portion, CD

$$T_{ECD} = \sum_{i=1}^{i=n_v} \int_{R_{i-1}}^{R_i} \int_0^{2\pi} \tau_{im+1} R dR d\varphi \quad (17)$$

where the torsion moment in portion, CD , is written as (Fig. 1)

$$T_{ECD} = \sum_{i=1}^{i=m} T_i \quad (18)$$

The strain, τ_{im+1} , is expressed as a function of shear strain, γ_{CD} , by using the stress-strain relation (9).

The distribution of γ in the cross-section of the external crack arm is written as

$$\gamma = \frac{\gamma_{CD}}{R_A} R \quad (19)$$

where

$$R_B \leq R \leq R_A \quad (20)$$

The equation obtained by substituting of (9), (18) and (19) in (17) should be solved with respect to γ_{CD} by using the MatLab computer program.

The following equation for equilibrium of the rod cross-section in portion, DP , is used to determine the shear strain, γ_{DP} , that participates in (13)

$$T_{UDP} = \sum_{i=1}^{i=n_{nc}} \int_{R_{i-1}}^{R_i} \int_0^{2\pi} \tau_{il} R dR d\varphi \quad (21)$$

where the torsion moment in rod portion, DP , is found as (Fig. 1)

$$T_{UDP} = \sum_{i=1}^{i=m} T_i + T_b \tag{22}$$

The stress-strain relation (9) is used to express the shear stress, τ_{i1} , as a function of shear strain, γ . The distribution of γ in the cross-section of the rod in portion, DP , is written as

$$\gamma = \frac{\gamma_{DP}}{R_A} R \tag{23}$$

where

$$0 \leq R \leq R_A \tag{24}$$

After substituting of (9), (22) and (23) in (21), the equation should be solved with respect to γ_{DP} by the MatLab computer program.

3. Numerical example

The general solution (13) derived in the previous section of this paper is applied here to analyze the strain energy release rate for the delamination crack in the multilayered inhomogeneous cantilever rod shown in Fig. 2. The cross-section of the rod is a circle of radius, R_A . The rod is made of an arbitrary number of adhesively bonded concentric longitudinal layers. A delamination circular crack of radius, R_B , and length, a , is located between layers. The length of the rod is l . The rod is clamped in its right-hand end. The loading of the rod consists of two torsion moments, T_1 and T_B , applied at the external crack arm and at the free end of the internal crack arm, respectively.

The non-linear mechanical behaviour of the material in the i -th layer of the rod is treated by the following stress-strain relation (Petrov, 2014)

$$\tau_i = E_i \gamma - H_i \gamma^{\alpha_i} - L_i \gamma^{\beta_i} \tag{25}$$

where τ_i is the shear stress, γ is the shear strain, E_i is the modulus of elasticity, H_i , L_i , α_i and β_i are material properties.

The material in each layer exhibits continuous material inhomogeneity in radial direction. The distribution of E_i in radial direction of the i -th layer is described by the following power law

$$E_i = E_{Q_i} + \frac{E_{M_i} - E_{Q_i}}{(R_i - R_{i-1})^{f_i}} (R - R_{i-1})^{f_i} \tag{26}$$

where

$$R_{i-1} \leq R \leq R_i \tag{27}$$

In (26), E_{Q_i} and E_{M_i} are the values of E_i at the internal and external surfaces of the layer, f_i is a material property that controls the material inhomogeneity.

For the rod in Fig. 2, one writes

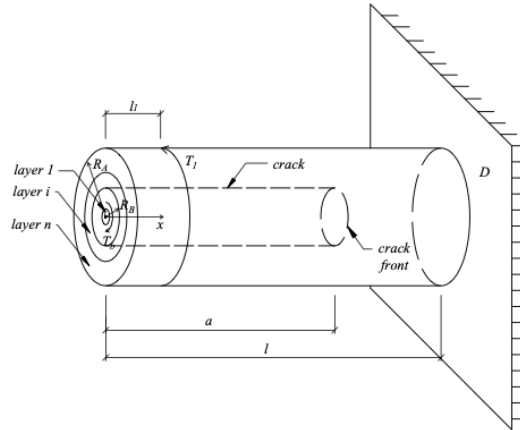


Fig. 2 Geometry and loading of a multilayered inhomogeneous cantilever rod

$$n_T = 1 \tag{28}$$

Therefore, the solution to the strain energy release rate (13) takes the form

$$G = \frac{T_1}{2\pi R_B} \left(\frac{\gamma_{CD}}{R_A} - \frac{\gamma_{DP}}{R_A} \right) + \frac{T_b}{2\pi R_B} \left(\frac{\gamma_{br}}{R_B} - \frac{\gamma_{DP}}{R_A} \right) - \frac{1}{2\pi R_B} \left[\sum_{i=1}^{i=n_b} \int_{R_{i-1}}^{R_i} \int_0^{2\pi} u_{0br_i} R dR d\varphi + \sum_{i=1}^{i=n_n} \int_{R_{i-1}}^{R_i} \int_0^{2\pi} u_{0vni_{i+1}} R dR d\varphi - \sum_{i=1}^{i=n_c} \int_{R_{i-1}}^{R_i} \int_0^{2\pi} u_{0nc_{i1}} R dR d\varphi \right] \tag{29}$$

The shear strain, γ_{br} , that is involved in (29) is obtained from the Eq. (14). After substituting of (15), (25) and (26) in (14), the equation is solved with respect to γ_{br} by the MatLab computer program. Equation (17) is used to determine the shear strain, γ_{CD} , that is involved in (29). For this purpose, by using (18), the torsion moment, T_{ECD} , is found as

$$T_{ECD} = T_1 \tag{30}$$

Then, the equation obtained by substituting of (19), (25), (26) and (30) in (17) is solved with respect to γ_{CD} by the MatLab computer program. The shear strain, γ_{DP} , that that is involved in (29) is determined by equation (21). By applying (22), the torsion moment is obtained as

$$T_{UDP} = T_1 - T_b \tag{31}$$

After substituting of (23), (25), (26) and (31) in (21), the equation is solved with respect to γ_{DP} by the MatLab computer program.

The strain energy density, u_{0br_i} , that is involved in (29) is obtained by substituting of (25) in (10). The result is

$$u_{0br_i} = \frac{E_i \gamma^2}{2} - \frac{H_i \gamma^{\alpha_i+1}}{\alpha_i + 1} - \frac{L_i \gamma^{\beta_i+1}}{\beta_i + 1} \tag{32}$$

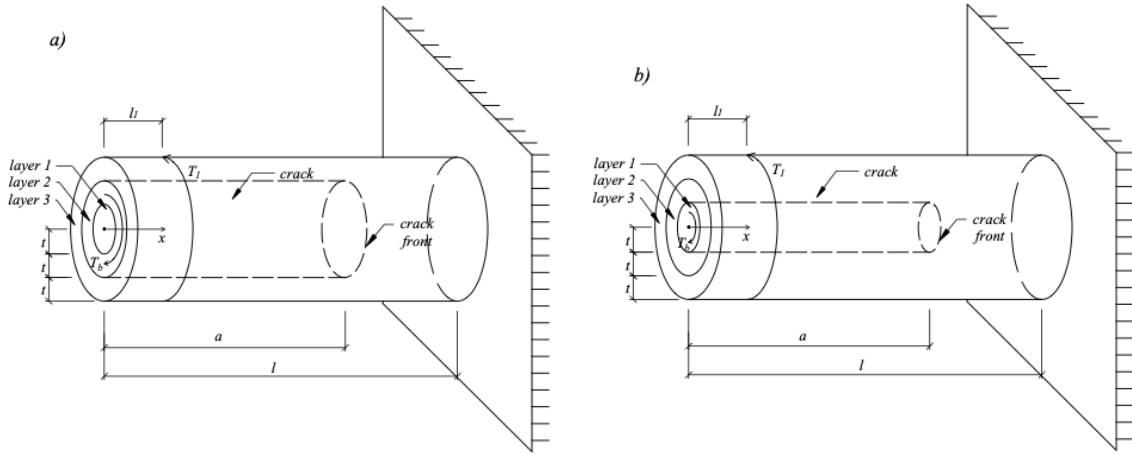


Fig. 3 Two three-layered inhomogeneous cantilever rods with a delamination circular cylindrical crack located between (a) layers 2 and 3 and (b) layers 1 and 2

Eq. (32) is used also to derive $u_{0vn_{m+1}}$. For this purpose, γ is replaced with γ_{CD} . The strain energy density, $u_{0nc_{i1}}$, is obtained by replacing of γ with γ_{DP} in (32).

After substituting of γ_{br} , γ_{m+1} , γ_{s_1} , u_{0br_i} , $u_{0vn_{m+1}}$ and $u_{0nc_{i1}}$ in (29), the integration is carried-out by the MatLab computer program.

In order to verify (29), the strain energy release rate is derived also by differentiating the complementary strain energy with respect to the crack area

$$G = \frac{dU^*}{l_{cf} da} \tag{33}$$

where da is an elementary increase of the crack length, U^* is the complementary strain energy. By substituting of (3) in (33), one obtains

$$G = \frac{dU^*}{2\pi R_B da} \tag{34}$$

The complementary strain energy is expressed as

$$U^* = \sum_{i=1}^{i=n_b} \int_0^a \int_{R_{i-1}}^{R_i} \int_0^{2\pi} u_{0br_i}^* R dR d\varphi + \sum_{i=1}^{i=n_v} \int_{l_1}^a \int_{R_{i-1}}^{R_i} \int_0^{2\pi} u_{0vn_{m+1}}^* R dR d\varphi + \sum_{i=1}^{i=n_c} \int_a^l \int_{R_{i-1}}^{R_i} \int_0^{2\pi} u_{0nc_{i1}}^* R dR d\varphi \tag{35}$$

where $u_{0br_i}^*$, $u_{0vn_{m+1}}^*$ and $u_{0nc_{i1}}^*$ are the complementary strain energy densities in the i -th layers of the internal and external crack arms, and the un-cracked part of the rod, respectively, l_1 is the abscissa of the cross-section in which the torsion moment, T_1 , is applied (Fig. 2).

Since the complementary strain energy density is equal to the area that complements the area enclosed by the stress-strain curve to a rectangle, the complementary strain energy density in the i -th layer of the internal crack arm is written as

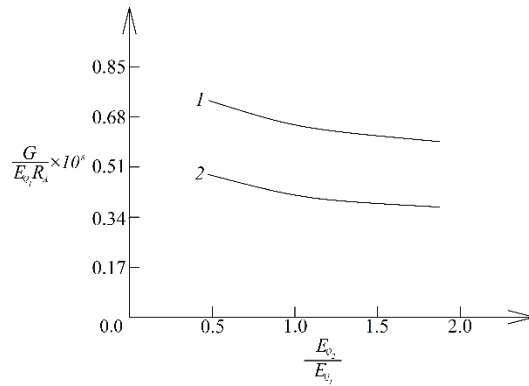


Fig. 4 The strain energy release rate in non-dimensional form plotted against E_{Q_2}/E_{Q_1} (curve 1 – for the three-layered rod configuration with a delamination crack between layers 2 and 3 (Fig. 3a), curve 2 – for the three-layered rod configuration with a delamination crack between layers 1 and 2 (Fig. 3b))

$$u_{0br_i}^* = \tau_i \gamma - u_{0br_i} \tag{36}$$

By substituting of (25) and (32) in (36), one derives

$$u_{0br_i}^* = \frac{E_i \gamma^2}{2} - \frac{\alpha_i H_i \gamma^{\alpha_i + 1}}{\alpha_i + 1} - \frac{\beta_i L_i \gamma^{\beta_i + 1}}{\beta_i + 1} \tag{37}$$

Eq. (37) is applied also in order to obtain the complementary strain energy density in the i -th layer of the external crack arm. For this purpose, γ is replaced with γ_{CD} . The complementary strain energy density in the i -th layer of the un-cracked part of the rod is found by replacing of γ with γ_{DP} in (37).

By substituting of (35) in (34), one obtains the following expression for the strain energy release rate for the delamination crack in the cantilever rod shown in Fig. 2

$$G = \frac{1}{2\pi R_B} \left[\sum_{i=1}^{i=n_b} \int_{R_{i-1}}^{R_i} \int_0^{2\pi} u_{0br_i}^* R dR d\varphi + \sum_{i=1}^{i=n_v} \int_{R_{i-1}}^{R_i} \int_0^{2\pi} u_{0vni_{m+1}}^* R dR d\varphi - \sum_{i=1}^{i=n_c} \int_{R_{i-1}}^{R_i} \int_0^{2\pi} u_{0nc_{i1}}^* R dR d\varphi \right] \tag{38}$$

The integration in (38) is carried-out by the MatLab computer program. It should be noted that the strain energy release rate obtained by (38) is exact match of that found by (29). This fact is a verification of the delamination fracture analysis of the inhomogeneous multilayered non-linear elastic rod developed in the present paper.

The solution to the strain energy release rate (38) is applied in order to evaluate the effects of the material inhomogeneity, the crack location in radial direction and the non-linear mechanical behaviour of the material on the delamination fracture in the inhomogeneous multilayered cantilever rod configuration. The strain energy release rate is presented in non-dimensional form by using the formula $G_N = G/(E_{Q_1} R_A)$. In order to evaluate the effect of crack location in radial direction on the fracture behaviour, two three-layered cantilever rod configurations are analyzed (Fig. 3). A delamination circular cylindrical crack of length, a , is located between layers 2 and 3 in the rod shown in Fig. 3(a). A three-layered rod configuration with a delamination circular

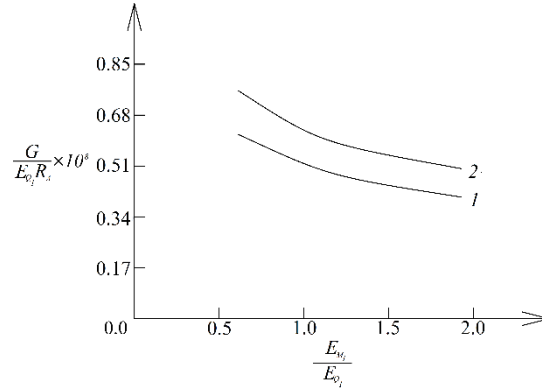


Fig. 5 The strain energy release rate in non-dimensional form plotted against E_{M1} / E_{Q1} ratio (curve 1 – at linear-elastic behaviour of the material, curve 2 – at non-linear behaviour of the material)

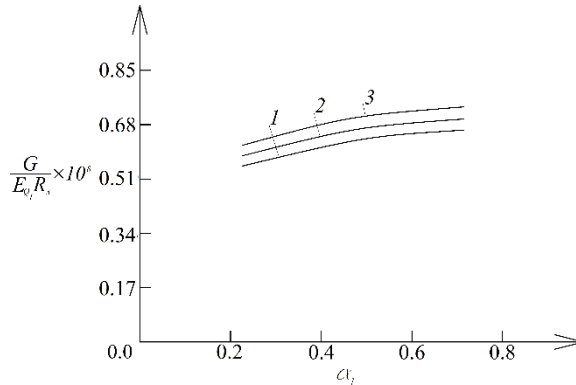


Fig. 6 The strain energy release rate in non-dimensional form plotted against α_1 (curve 1 - at $H_1 / E_{Q1} = 0.066$, curve 2 – at $H_1 / E_{Q1} = 0.132$ and curve 3 – at $H_1 / E_{Q1} = 0.200$)

cylindrical crack of length, a , located between layers 1 and 2 is also considered (Fig. 3(b)). The thickness of each layer in both rod configurations is t (Fig. 3). Both rods are clamped in their right-hand ends. The loading of the rods consists of two torsion moments, T_b and T_1 , where T_b is applied at the free end of the internal crack arm. The external crack arm is loaded by the torsion moment, T_1 , applied at distance, l_1 , from the free end of the rod (Fig. 3). It is assumed that $t=0.004$ m, $l=0.250$ m. $T_1=12$ Nm and $T_b=5$ Nm.

The effect of the crack location in radial direction on the delamination fracture behaviour is illustrated in Fig. 4 where the strain energy release rate in non-dimensional form is plotted against E_{Q2} / E_{Q1} ratio for both three-layered rod configurations shown in Fig. 3. It is assumed that

$$\begin{aligned}
 & E_{M1} / E_{Q1} = 0.3, \quad H_1 / E_{Q1} = 0.2, \quad L_1 / E_{Q1} = 0.1, \quad f_1 = 0.5, \quad \alpha_1 = 0.7, \quad \beta_1 = 0.6, \\
 & E_{M2} / E_{Q2} = 0.4, \quad H_2 / E_{Q2} = 0.3, \quad L_2 / E_{Q2} = 0.1, \quad f_2 = 0.5, \quad \alpha_2 = 0.7, \quad \beta_2 = 0.6, \\
 & E_{Q3} / E_{Q1} = 0.5, \quad E_{M3} / E_{Q3} = 0.3, \quad H_1 / E_{Q3} = 0.1, \quad f_3 = 0.5, \quad \alpha_3 = 0.7 \text{ and } \beta_3 = 0.6.
 \end{aligned}$$

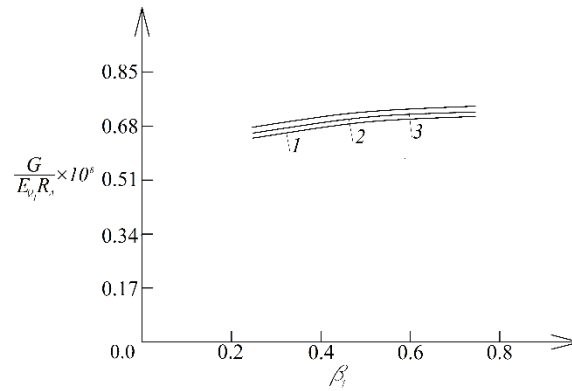


Fig. 7 The strain energy release rate in non-dimensional form plotted against β_1 (curve 1 – at $L_1/E_{Q_1}=0.033$, curve 2 – at $L_1/E_{Q_1}=0.066$ and curve 3 – at $L_1/E_{Q_1}=0.100$)

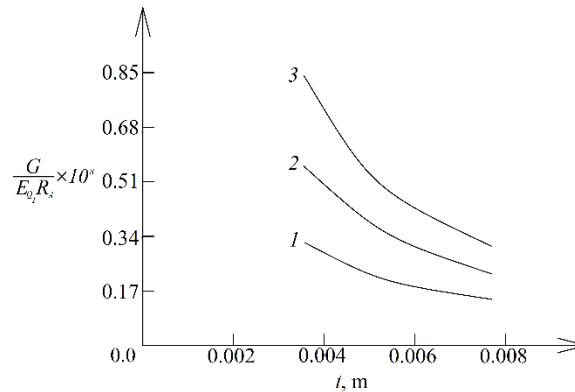


Fig. 8 The strain energy release rate in non-dimensional form plotted against the layer thickness, t (curve 1 – at $T_1=7.2$ Nm and $T_b=3$ Nm, curve 2 – at $T_1=9.6$ Nm and $T_b=4$ Nm, and curve 3 – at $T_1=12$ Nm and $T_b=5$ Nm)

The curves in Fig. 4 indicate that the strain energy release rate is higher when the crack is located between layers 2 and 3. This finding is attributed to the fact that when the crack is located between layers 2 and 3 (Fig. 3(a)) the stiffness of the external crack arm, which is loaded by a torsion moment of a higher magnitude, is lower in comparison with the case when the crack is located between layers 1 and 2 (Fig. 3(b)). One can observe also in Fig. 4 that the strain energy release rate decreases with increasing of E_{Q_2}/E_{Q_1} ratio (this behaviour is due to increase of the stiffness of the rod).

The effect of material inhomogeneity in radial direction of layer 1 on the delamination fracture behaviour is evaluated too. The material inhomogeneity in radial direction of layer 1 is characterized by E_{M_1}/E_{Q_1} ratio. Thus, in order to evaluate the effect of material inhomogeneity, calculations of the strain energy release rate are carried-out at various E_{M_1}/E_{Q_1} ratios. The three-layered inhomogeneous cantilever rod configuration with delamination crack located between layers 2 and 3 is considered (Fig. 3(a)).

One can get an idea for the effect of E_{M_1}/E_{Q_1} ratio on the delamination fracture behaviour from

Fig. 5 where the strain energy release rate in non-dimensional form is plotted against E_{M_1}/E_{Q_1} ratio. It is evident from Fig. 5 that the strain energy release rate decreases with increasing of E_{M_1}/E_{Q_1} ratio. The effect of the non-linear mechanical behaviour of the inhomogeneous material on the delamination fracture is evaluated also. For this purpose, the strain energy release rate derived assuming linear elastic mechanical behaviour of the material is plotted in non-dimensional form against E_{M_1}/E_{Q_1} ratio in Fig. 5 for comparison with the non-linear solution. It should be mentioned that the linear-elastic solution to the strain energy release rate is derived by substituting of $H_i=0$ and $L_i=0$ in the non-linear solution (38) since at $H_i=0$ and $L_i=0$ the non-linear stress-strain relation (25) transforms into the Hooke's law assuming that E_i is the modulus of elasticity of the inhomogeneous material in the i -th layer of the rod. It can be observed in Fig. 5 that the non-linear mechanical behaviour of the material leads to increase of the strain energy release rate.

The influence of H_1/E_{Q_1} ratio and material property, α_1 , on the delamination fracture behaviour is investigated. The rod configuration with delamination crack located between layers 1 and 2 is considered (Fig. 3(a)). The strain energy release rate in non-dimensional form is plotted against α_1 in Fig. 6 at three H_1/E_{Q_1} ratios. The curves shown in Fig. 6 indicate that the strain energy release rate increases with increasing of α_1 . It can be observed also in Fig. 6 that the strain energy release rate increases with increasing of H_1/E_{Q_1} ratio.

The influence of material property, β_1 , and L_1/E_{Q_1} ratio on the delamination fracture behaviour is also investigated. The three-layered rod with crack between layers 2 and 3 is under consideration. Calculations of the strain energy release rate are carried-out at various values of β_1 . The results obtained are presented in Fig. 7 where the strain energy release rate in non-dimensional form is plotted against β_1 at three L_1/E_{Q_1} ratios. One can observe in Fig. 7 that increase of β_1 leads to increase of the strain energy release rate. The curves in Fig. 7 indicate also that the strain energy release rate increases with increasing of L_1/E_{Q_1} ratio.

The influence of the thickness of the layers, t , on the delamination fracture behaviour is analyzed. The influence of the loading conditions is analyzed too. The rod with delamination crack located between layers 2 and 3 is considered (Fig. 3(a)). The strain energy release rate is calculated at various values of t at $T_1=7.2$ Nm and $T_b=3$ Nm, $T_1=9.6$ Nm and $T_b=4$ Nm, and $T_1=12$ Nm and $T_b=5$ Nm. The influences of the thickness of the layers and the values of the torsion moments on the delamination fracture behaviour of the rod are illustrated in Fig. 8 where the strain energy release rate in non-dimensional form is plotted against t at $T_1=7.2$ Nm and $T_b=3$ Nm, $T_1=9.6$ Nm and $T_b=4$ Nm, and $T_1=12$ Nm and $T_b=5$ Nm. It is evident from the curves in Fig. 8 that the strain energy release rate decreases with increasing of the thickness, t . The curves in Fig. 8 indicate also that the strain energy release rate increases with increasing of the magnitudes of the torsion moments applied on the rod.

4. Conclusions

Delamination fracture behaviour of inhomogeneous multilayered rod configurations of circular cross-section is analyzed.

The rods are made of adhesively bonded concentric longitudinal layers. A delaminating crack presenting a circular cylindrical surface is located arbitrary between layers. The internal crack arm has a circular cross-section. Thus, the delamination crack front is a circle. The external crack arm

has a ring-shaped cross-section. The rods are loaded by torsion moments. The internal crack arm is loaded by a torsion moment applied at the free end. Each layer exhibits continuous (smooth) material inhomogeneity in radial direction. Besides, the material has non-linear elastic mechanical behaviour. The delamination fracture behaviour of the rods is studied in terms of the strain energy release rate. For this purpose, general solution to the strain energy release rate is derived by considering the balance of the energy. The solution is valid for rods made of an arbitrary number of concentric longitudinal layers. Besides, each layer has individual thickness and material properties. The solution holds for arbitrary law for continuous distribution of the material properties in radial direction. The solution is used to analyze the delamination fracture of an inhomogeneous multilayered non-linear elastic cantilever rod configuration loaded in torsion. The strain energy release rate for the delamination crack in the cantilever rod is derived also by considering the complementary strain energy for verification. The solution is applied to investigate the effects of material inhomogeneity in radial direction, the loading conditions, the non-linear mechanical behaviour of the material and the crack location in radial direction on the delamination fracture. The analysis reveals that the strain energy release rate decreases with increasing of E_{M_1}/E_{Q_1} ratio. It is found also that the non-linear mechanical behaviour of the material leads to increase of the strain energy release rate. The calculations show that the strain energy release rate increases with increasing of H_1/E_{Q_1} and L_1/E_{Q_1} ratios. The increase of α_1 and β_1 leads also to increase of the strain energy release rate. Concerning the effect of the thickness of the layers on the delamination fracture behaviour, it is found that the strain energy release rate decreases with increasing of the thickness.

References

- Carpinteri, A. and Pugno, N. (2006), "Cracks in re-entrant corners in functionally graded materials", *Eng. Fract. Mech.*, **73**(6), 1279-1291. <https://doi.org/10.1016/j.engfracmech.2006.01.008>.
- Dolgov, N.A. (2005), "Determination of stresses in a two-layer coating", *Strength Mater.*, **37**(2), 422-431. <https://doi.org/10.1007/s11223-005-0053-7>.
- Dolgov, N.A. (2016), "Analytical methods to determine the stress state in the substrate-coating system under mechanical loads", *Strength Mater.*, **48**(1), 658-667. <https://doi.org/10.1007/s11223-016-9809-5>.
- Erdogan, F. (1995), "Fracture mechanics of functionally graded materials", *Comput. Eng.*, **5**(1), 753-770. [https://doi.org/10.1016/0961-9526\(95\)00029-M](https://doi.org/10.1016/0961-9526(95)00029-M).
- Gasik, M.M. (2010), "Functionally graded materials: bulk processing techniques", *Int. J. Mater. Prod. Technol.*, **39**(1-2), 20-29. <https://doi.org/10.1504/IJMPT.2010.034257>.
- Han, X., Xu, Y.G. and Lam, K.Y. (2001), "Material characterization of functionally graded material by means of elastic waves and a progressive-learning neural network", *Compos. Sci. Technol.*, **61**(10), 1401-1411. [https://doi.org/10.1016/S0266-3538\(01\)00033-1](https://doi.org/10.1016/S0266-3538(01)00033-1).
- Hedia, H.S., Aldousari, S.M., Abdellatif, A.K. and Fouda, N.A. (2014), "New design of cemented stem using functionally graded materials (FGM)", *Biomed. Mater. Eng.*, **24**(3), 1575-1588. <https://doi.org/10.3233/BME-140962>.
- Hirai, T. and Chen, L. (1999), "Recent and prospective development of functionally graded materials in Japan", *Mater. Sci. Forum*, **308-311**(4), 509-514. <https://doi.org/10.4028/www.scientific.net/MSF.308-311.509>.
- Kawasaki, A. and Watanabe, R. (1997), "Concept and P/M fabrication of functionally gradient materials", *Ceramics Int.*, **23**(1), 73-83. [https://doi.org/10.1016/0272-8842\(95\)00143-3](https://doi.org/10.1016/0272-8842(95)00143-3).
- Mahamood, R.M. and Akinlabi, E.T. (2017), *Functionally Graded Materials*, Springer.

- Markworth, A.J., Ramesh, K.S. and Parks Jr., W.P. (1995), "Review: modeling studies applied to functionally graded materials", *J. Mater. Sci.*, **30**(3), 2183-2193. <https://doi.org/10.1007/BF01184560>.
- Miyamoto, Y., Kaysser, W.A., Rabin, B.H., Kawasaki, A. and Ford, R.G. (1999), *Functionally Graded Materials: Design, Processing and Applications*, Kluwer Academic Publishers.
- Nemat-Allal, M.M., Ata, M.H., Bayoumi, M.R. and Khair-Eldeen, W. (2011), "Powder metallurgical fabrication and microstructural investigations of Aluminum/Steel functionally graded material", *Mater. Sci. Appl.*, **2**(5), 1708-1718. <https://doi.org/10.4236/msa.2011.212228>.
- Petrov, V.V. (2014), *Non-linear Incremental Structural Mechanics*, M.: Infra-Injeneria.
- Rizov, V. I. (2018a), "Non-linear longitudinal fracture in a functionally graded beam", *Coupled Syst. Mech.*, **7**(4), 441-453. <https://doi.org/10.12989/csm.2018.7.4.441>.
- Rizov, V.I. (2018b), "Non-linear fracture in bi-directional graded shafts in torsion", *Multidiscip. Model. Mater. Struct.*, **15**(1), 156-169. <https://doi.org/10.1108/MMMS-12-2017-0163>.
- Rizov, V.I. (2019), "Influence of sine material gradients on delamination in multilayered beams", *Coupled Syst. Mech.*, **8**(1), 1-17. <https://doi.org/10.12989/csm.2019.8.1.001>.
- Saiyathibrahim, A., Subramaniyan, R. and Dhanapl, P. (2016), "Centrifugally cast functionally graded materials—review", *Proceedings of the International Conference on Systems, Science, Control, Communications, Engineering and Technology*.
- Shrikantha Rao, S. and Gangadharan, K.V. (2014), "Functionally graded composite materials: an overview", *Procedia Mater. Sci.*, **5**(1), 1291-1299. <https://doi.org/10.1016/j.mspro.2014.07.442>.
- Tilbrook, M.T., Moon, R.J. and Hoffman, M. (2005), "Crack propagation in graded composites", *Compos. Sci. Technol.*, **65**(2), 201-220. <https://doi.org/10.1016/j.compscitech.2004.07.004>.
- Tokovyy, Y. and Ma, C.C. (2008), "Analysis of 2D non-axisymmetric elasticity and thermoelasticity problems for radially inhomogeneous hollow cylinders", *J. Eng. Math.*, **61**(3), 171-184. <https://doi.org/10.1007/s10665-007-9154-6>.
- Tokovyy, Y. and Ma, C.C. (2013), "Three-dimensional temperature and thermal stress analysis of an inhomogeneous layer", *J. Therm. Stresses*, **36**(2), 790-808. <https://doi.org/10.1080/01495739.2013.787853>.
- Tokova, L., Yasinsky, A. and Ma, C.C. (2017), "Effect of the layer inhomogeneity on the distribution of stresses and displacements in an elastic multilayer cylinder", *Acta Mechanica*, **228**(8), 2856-2877. <https://doi.org/10.1007/s00707-015-1519-8>.
- Tokovyy, Y. and Ma, C.C. (2016), "Axisymmetric stresses in an elastic radially inhomogeneous cylinder under length-varying loadings", *ASME J. Appl. Mech.*, **83**(11), 111-007-111-007-7. <https://doi.org/10.1115/1.4034459>.